Determination of site amplification, polarization and topographic effects in the seismic response of the Port Hills following the 2011 Christchurch earthquake

A. Kaiser, C. Holden & C. Massey

GNS Science, Avalon, Lower Hutt.

2013 NZSEE Conference

ABSTRACT: The Canterbury earthquake sequence provides an internationally significant case study to understand the influence of ground motion amplification effects in hillside areas. Severe ground failure and building damage occurred in the southern Port Hills suburbs of Christchurch during the Mw 6.2 February and Mw 6.0 June 2011 earthquakes. Damage patterns indicate that amplification of ground motions due to localised features has likely contributed to the most severe effects.

We present new seismological data collected by small-scale temporary arrays at four sites to characterise the seismic site response and assess the extent to which amplification from lithological and topographic factors influenced ground motions. Our initial analyses from records at two of the sites reveal significant complexity in ground motion amplification and polarization over small distances within our arrays for any given event. This supports the hypothesis that local topographic shape and/or lithology strongly influences ground motion in areas of highly variable topography. Our results have engineering implications, given that these effects are occurring in areas all classed as rock according to the New Zealand design standards (NZS1170) and much of New Zealand's population and infrastructure is built on hillside locations in areas with high seismic hazard (e.g. Wellington city).

1 INTRODUCTION

Current building codes broadly classify ground shaking hazard based on foundation soil conditions, with sites on rock assumed to have generally lower amplitude and higher frequency shaking (NZS1170). However, significant local variations in ground motion can arise within the rock site classes. Firstly, amplified ground motions can result from near-surface impedance contrasts associated with local surficial deposits (colluvium, alluvium etc) or highly fractured material overlying more intact materials (that may be associated with landslide-prone slopes). Secondly, focusing of seismic waves by surface topography may result in topographic amplification. This phenomenon led to greater building damage on a prominent ridge top than at nearby soft soil sites in the 2010 Haiti earthquake (Hough et al., 2010). Furthermore the shape of lithologic and topographic structures can lead to directivity effects, where ground motion is preferentially polarised in a given direction (e.g. Bonamassa & Vidale 1991; Del Gaudio & Wasowski 2010).

Previous seismological studies have inferred that localised amplification effects can have substantial control on the patterns and concentration of building, landslides and ground damage on slopes (e.g. Harp & Jibson 2002; Sepúlveda et al. 2005; Meunier et al. 2008; Buech et al. 2010; Hough et al. 2010). Given that such amplification effects are not taken into account in current earthquake design practice, more research is needed to understand their importance, in order to guide future seismic hazard mitigation efforts.

Severe ground failure and building damage occurred in the southern Port Hills suburbs of Christchurch during the Mw 6.2, 22 February and Mw 6.0, 13 June 2011 earthquakes (Figure 1). Field inspections indicate localised high levels of damage associated with landslide activity and/or topographic shape. Accordingly, we have collected new seismological data using small-scale temporary GeoNet arrays at four locations to characterise the seismic site response and assess the extent to which amplification

influenced ground motions. All of these sites would be classified as rock or weak rock (Site class B) under NZS1170. Here, we present preliminary observations for two small-scale seismometer arrays at Kinsey Terrace and Mount Pleasant, focusing on identification of ground motion amplification and polarization effects. To do this we analyse azimuthal arias intensity (a parameter often correlated with slope failure) and investigate the corresponding frequency contributions. In-depth quantification of local site effects for all arrays will be conducted at a later stage.

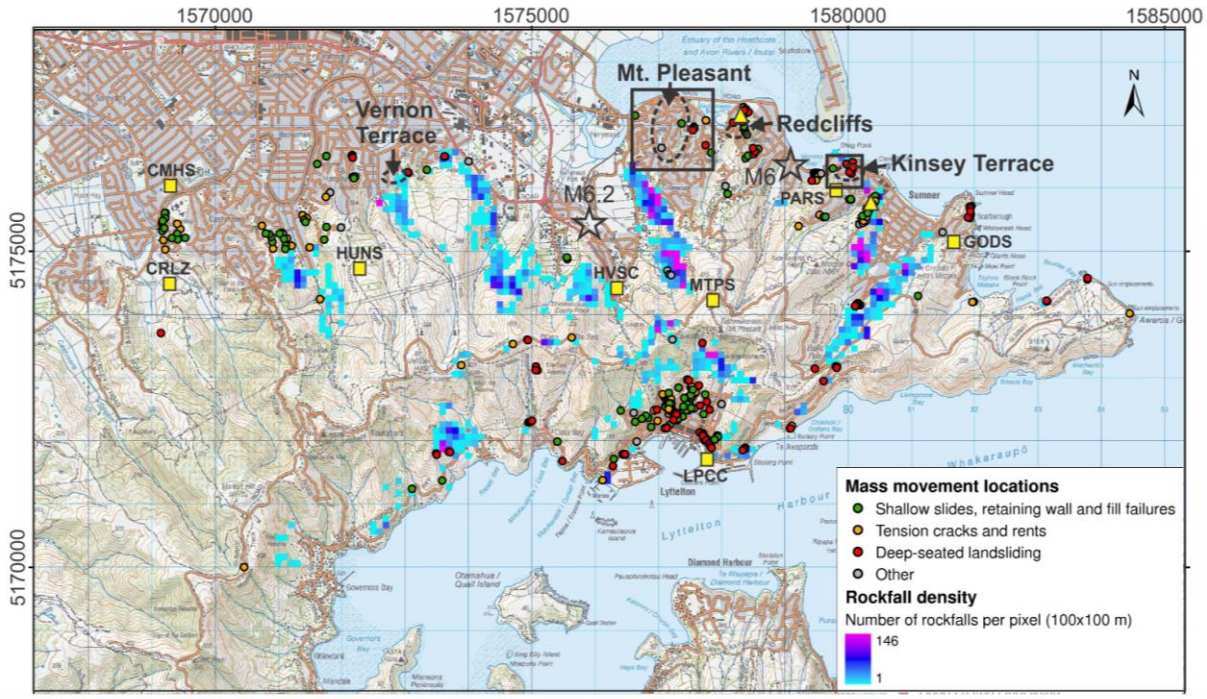

Figure 1: Map showing the location of four temporary seismometer arrays (dashed black ellipses) and distribution of mass movements, including rockfall density following the 22 February Christchurch earthquake. Data was collated from information collected by the Engineering Geology response team at GNS Science, the Port Hills Geotechnical Group and Zealand Aerial Mapping. Coordinates are in New Zealand Map Grid (m). Yellow squares are permanent GeoNet strong-motion stations; triangles are the locations of two recently installed borehole strong motion stations. The rectangles refer to the area shown in Figure 3. The epicentres of the M 6.2 February and M 6 June earthquakes are shown as stars.

2 PORT HILLS SEISMIC ARRAYS

The Port Hills form the flanks of the outcropping extinct volcano of Banks Peninsula (up to 500m above sea level). These volcanic rocks belong to the Lyttelton Volcanic Group of Miocene age (10 – 12 Myrs old; Forsyth et al. 2008) and are mantled by much younger soils derived from wind-blown sand and silt (loess) and colluvial deposits of mixed rock and re-worked loess (Bell and Trangmar, 1987). These deposits are typically about 1 m thick and locally more than 5 m thick (Bell and Trangmar, 1987). Figure 1 maps the nature and distribution of ground failures in the hillside suburbs following the 22 February Christchurch earthquake. Major damage from the earthquake included: rockfalls; loess slides, falls and flows; loess and rock slides, falls and flows (e.g. Kinsey Terrace); rock slides, topples, falls and avalanches (e.g. Redcliffs) and toe slumps (e.g. Vernon Terrace).

Following the Mw 6.2 February 2011 earthquake, 1 Hz short-period sensors were deployed by GNS Science in small-scale temporary aftershock arrays at four key hillside sites (Figure 1). The geology and topography of these sites is described in Table 1 and Figure 2 respectively. Together, the arrays have recorded more than 1000 small to moderate-sized earthquakes.

First we look at data from the Kinsey Terrace array (Kinsey), an area of complex deformation in both loess and rock. Here coseismic permanent displacements recorded by continuous GPS and cadastral surveys (total horizontal displacement of ~1 m) appear to be primarily sub-parallel and down dip of

the volcanic sequences (towards bearing 070°-080°), suggesting a low-angle translational failure mechanism within the rock or at the loess/rock interface. Many of the residential properties on the displaced area show significant damage.

We then compare these results with the Mount Pleasant array located on a rock slope overlain by mixed loess and colluvial deposits. Here, no evidence of large permanent ground failure was observed, even though residential properties and retaining walls were significantly damaged by earthquake shaking.

Table 1: Description of the Port Hills seismic arrays

Array	Local Geology/Topography	Date In	Date out
Mt. Pleasant	A north-south trending ridgeline formed in mixed volcanic rocks thinly mantled with loess, fill and colluvium (< 1 m thick). High shaking damage to residential houses – no observed large scale mass movements	10.03.2011	31.03.2011
Redcliffs	A north-south trending ridgeline terminating in a steep (>60°) now abandoned coastal cliff, formed in mixed volcanic rocks. Cliff edge corresponds to a sharp break in slope. Significant shaking damage to houses located near break in slope	31.03.2011	27.04.2011
Vernon Terrace	Low angle slopes (~25°) near the valley bottom formed in mixed colluvium, loess and alluvium. Some shaking damage to houses but many damaged due to permanent ground deformation.	27.04.2011	09.06.2011
Kinsey Terrace	A north-south trending ridgeline terminating in a steep (>60°) now abandoned coastal cliff, formed in mixed volcanic rocks overlain by thick deposits (6-8 m in parts) of mainly loess. Deformation is towards the east and extends from below the ridge crest to the cliff edge. Many houses damaged due to permanent ground deformation.	09.06.2011	19.01.2012

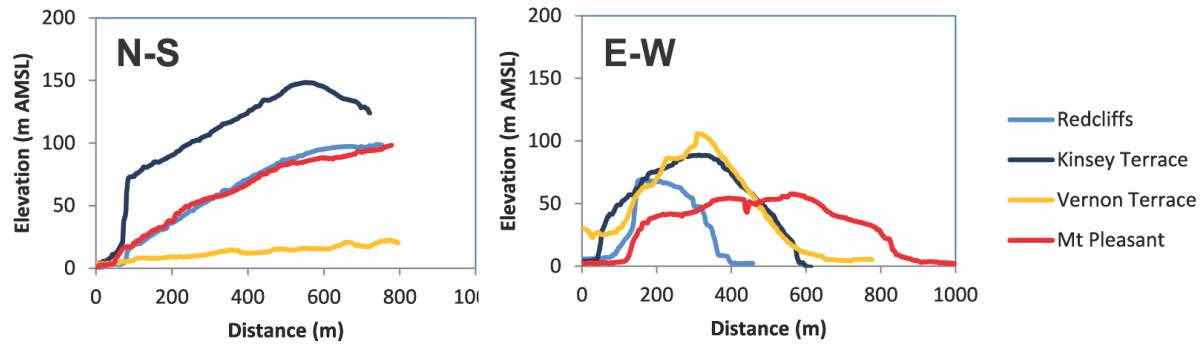

Figure 2 : Topographic cross sections north-south and east-west through each site array. Topography taken from the June 2011 LiDAR survey.

3 ARIAS AND FREQUENCY ANALYSIS OF THE KINSEY ARRAY DATA

The Kinsey array stations (labelled K1 to K5) are distributed on an E-W transect across the area of significant landslide movement (Figure 3). K1, K2 and K3 are located within the active deformation area, distributed from the toe (K1) to the crest (K3) of the area. K4 and K5 are located towards the crest of the ridge, beyond the area of deformation. A sharp cliff, striking east-west is located about 60 m north of the array. However, the direction of landslide movement was downslope towards the east (bearing 070°-080°) in the same orientation as the slope. The array dataset consists of 488 events that were recorded by all stations.

Figure 3: left: Kinsey Terrace small-scale array (red squares are seismometers) spanning an area of significant ground deformation. Right: Mount Pleasant small-scale seismometer array showing location of stations M1 – M5. White lines are the section locations mentioned in Figure 2.

We present preliminary arias intensity analyses of a selection of five events with various magnitudes (M2.5 to M4.3) and source azimuthal distributions. Figure 4 shows the contribution of different frequency bands to the overall arias intensity. Figure 5 shows the azimuthal polarization of arias intensity. We do not include station K2 because of unexplained and extreme lack of energy on the east component, which could be due to recording problems. However, K2 exhibits similar amplification characteristics to K1 and K3 on the north component.

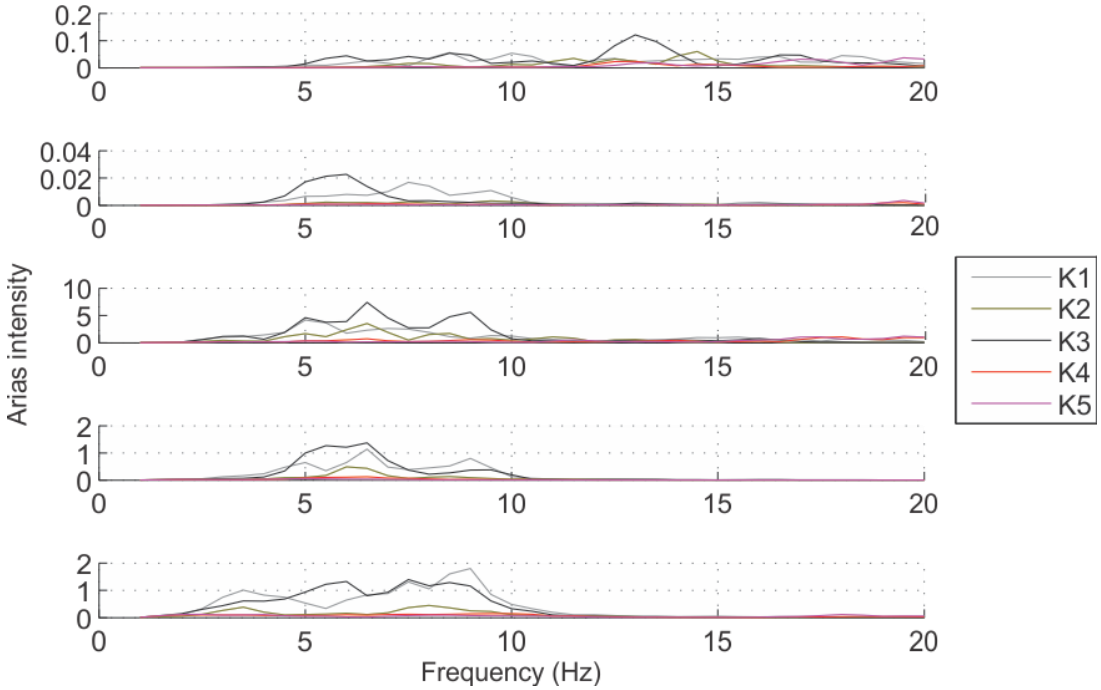

Figure 4: Maximum arias intensity within various frequency bands (calculated for narrow band-pass filtered data) for selected events recorded by the Kinsey array. Note, that the values for K2 are based solely on the maximum in the northwards direction. Also note that the vertical scale differs for each event.

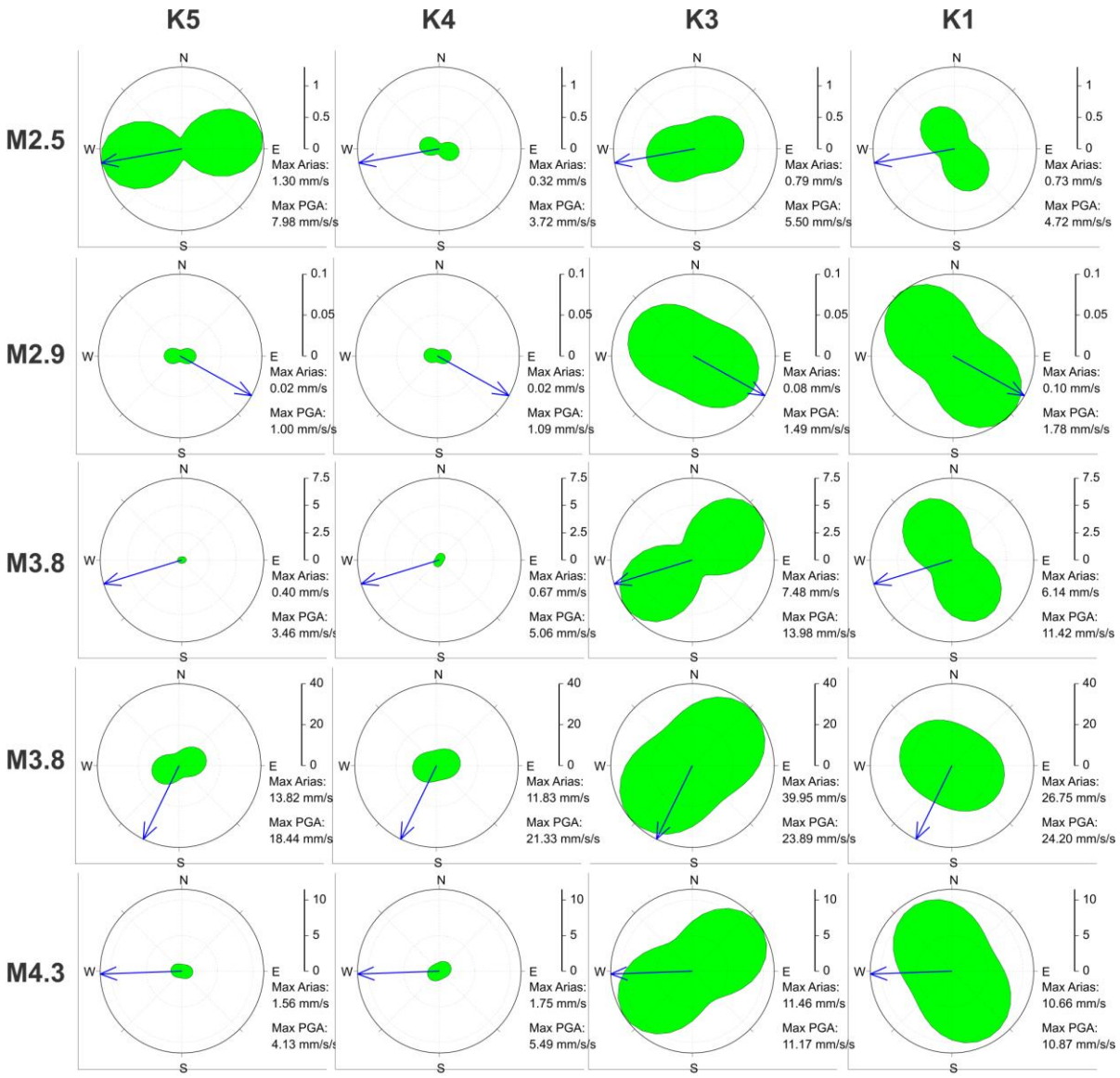

Figure 5: Arias intensity polar plots for Kinsey sites and sample events (increasing magnitudes from top to bottom). Arias intensity is calculated for various rotations of the recording axis system and normalized to the maximum value for a given event. The blue arrow points towards the earthquake epicentre.

Figures 4 and 5 show that for all events (except M2.5), stations K1, K2 and K3 exhibit much higher maximum arias intensities than K4 and K5 by factors of 3 to 5. Given that the first three stations are within the main body of deformation, this effect could largely be due to amplification within the disturbed material associated with the displacement. We observe that K3 shows a consistently large contribution to arias intensity from the 6 Hz band for all magnitudes and azimuths (Figure 4), indicating that there is likely some site resonance at this frequency. Potential site resonances for other stations exist (e.g. ~10 Hz at K1), but are not well separated from source effects in these preliminary analyses.

In addition, topographic shapes of local structures may also be contributing to amplified ground motions. Figure 5 shows that for stations K3, K4 and K5 the maximum arias intensities were oriented within a narrow azimuth interval (predominantly northeast to east), corresponding to the local steepest-slope orientation, the main bearing of displacement (070°-080°) and the general dip direction of the volcanic sequence. Previous studies have postulated that such polarization is due to the reduction of the effective rock stiffness in a direction perpendicular to the dominant fracture orientation (e.g. Burjánek et al. 2010). However, station K1 shows a consistently different polarization for the maximum arias intensity (towards the northwest), regardless of earthquake back-azimuth. This direction is perpendicular to the steepest-slope orientation and main bearing of displacement,

suggesting localised complexity in the response. These data suggest that polarisation at K3 to K5 could be due to local slope orientation and the dip direction of the volcanic sequence, but at K1 the local shape of a northeast trending spur beneath the station could be influencing ground motions.

4 ARIAS AND FREQUENCY ANALYSIS OF THE MOUNT PLEASANT ARRAY DATA

The Mount Pleasant array stations (M1 – M5) are distributed along the top and side of a broad north-south striking ridge, that slopes gently downwards towards the north (Figure 3). All stations are located on volcanic rock, with only a thin (typically <1 m) cover of soil (e.g. loess, fill, colluvium). M1 is located at the toe of the north-south striking slope. M3 is located at the crest of the ridge at the break in slope between the steeper northern slope and the flatter southern slope, and M5 is located on the flat top of the ridge. M2 is located on the side of the ridge at the local crest of an abandoned sea cliff, marking sharp break-in-slope. M4 is in a local valley. In general, the station spacing (> 200 m) at this array is greater than at the other Port Hills arrays. The Mount Pleasant array recorded a total of 227 events at all five stations. We present arias intensity polar plots and frequency analyses for four selected events with various magnitudes and azimuthal distributions (Figures 6 and 7).

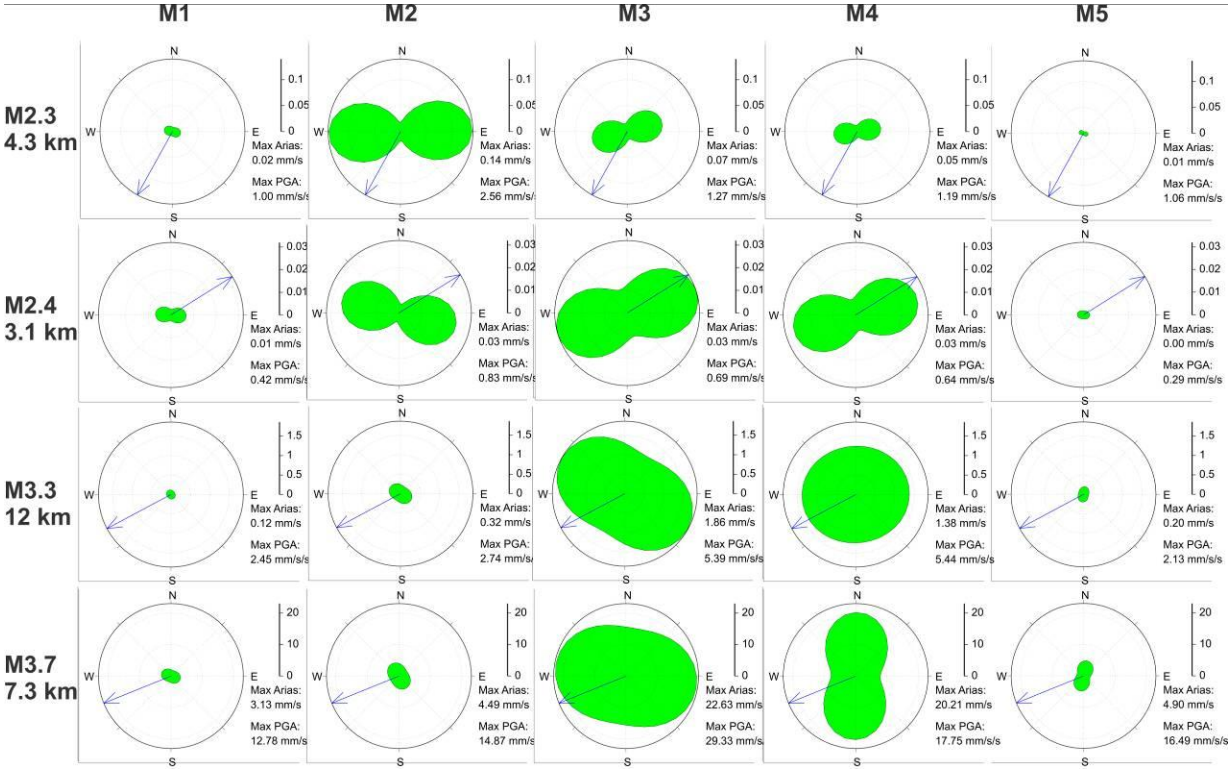

Figure 6: Arias polar plots for Mount Pleasant array for four sample events ranging from M 2.3 to M 3.7 (top to bottom). Arias intensity is calculated for various rotations of the recording axis system and normalized to the maximum value for a given event. Blue arrow is pointing towards the earthquake epicentre.

M3 (ridge crest) and M2 (local crest) show larger arias intensity amplifications up to a factor of 5with respect to M1 (slope toe) and M5 (flatter slope above ridge crest). Ground motion polarization in our data subset is generally E-W, with the exception of M5 in the south, perpendicular to the N-S trend of the ridge. These data suggest topography may be controlling the arias amplification at these sites (as in Buech et al. 2010; Hough et al.2010). We note, M4 is located on soil at the base of the hill, hence it is likely to have a different site response that is controlled by soil/basin-edge amplification effects.

The relative amplification is also clear on Figure 7. What is striking from Figure 7 is that the ground motion appears to be strongly resonant at different frequencies at each of these amplified sites (6 Hz at M4, 10 Hz at M3 and also > 15 Hz at M2 during the smaller local earthquakes). This resonance is consistent across all events and quite different from the source-dominated frequency plots shown for the Kinsey array. The high resonant frequencies suggest that these effects are occurring locally, from either small-scale lithological/topographic structures or man-made features. More investigation is

currently being carried out to understand the complex amplification patterns observed on this array and determine the likely causes.

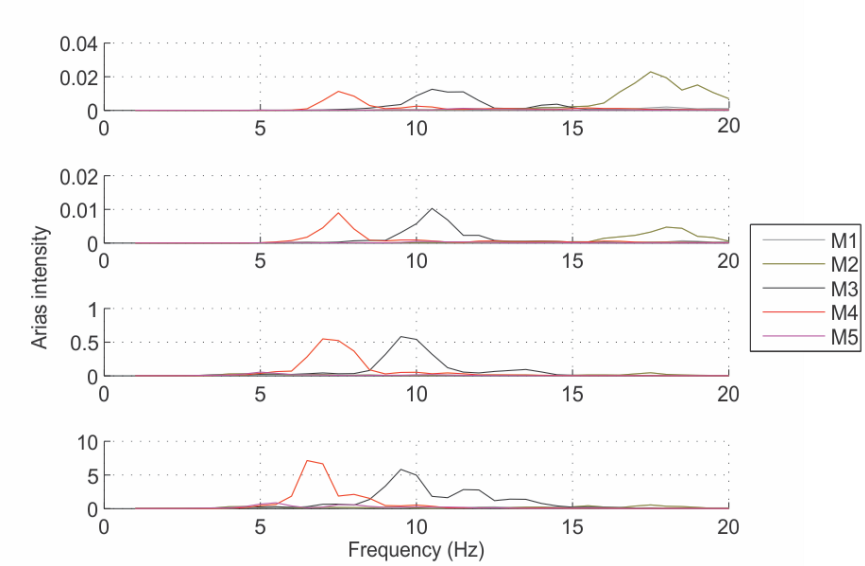

Figure 7: Maximum arias intensity for various frequency bands for selected events recorded at the Mount Pleasant array; Note, that the vertical scale differs for each event.

5 DISCUSSION AND CONCLUSIONS

The broad objective of this study was to better understand the localised site response to small and large earthquakes caused by variations in topography and lithology, and the link to damage patterns during the Canterbury events. We collected over 1,000 aftershocks following the February 2011 Christchurch earthquake, at four small-scale arrays located within the Port Hills. In this paper we present preliminary analyses of data from two arrays 1) Mount Pleasant, and 2) Kinsey Terrace. The main difference between the two sites was that at Kinsey Terrace the hillside showed significant coseismic permanent displacements over a relatively large area, whilst at Mt Pleasant there was only small-scale localised failures of retaining walls and cut slopes. However, both of these areas experienced significant ground accelerations during the 2010/2011 earthquake sequence, causing significant damage to buildings and infrastructure.

At Kinsey Terrace, our array transects an area of surface deformation where total permanent coseismic displacements of greater than 1 m were recorded. Stations located within the mapped deformation area exhibit strong amplification effects (3 to 5 times) compared to those sites (K4 and K5) on undamaged land further up the slope. A dominant resonant frequency of 6 Hz is especially strong at the site within the main body of the damage zone (K3), and could be associated with contrasting materials at depth within the area of deformation. The directivity of the dynamic response does not appear to be specific only to the area of deformation. For stations K3, K4 and K5 the maximum arias intensities were polarised within a narrow azimuth interval (predominantly northeast to east), corresponding to the local steepest-slope orientation, the main bearing of coseismic permanent displacement (070°-080°) and the general dip direction of the volcanic sequence. At station K1, at the toe of the deformation zone, consistently different polarization of ground motion occurred orientated perpendicular to that at the other stations. This indicates an alternative amplification mechanism, possibly associated with a local northeast trending spur.

At Mount Pleasant, our array is located on an N-S trending slope where significant shaking damage occurred to houses, especially in locations with similar topographic settings to stations M2 and M3. M2 and M3 are both located on convex breaks-in-slope where amplification factors were up to 5 times those recorded by stations M1 located at the slope toe, and M5, on the flatter area above the slope crest. The amplification pattern and general E-W polarization, suggest these effects are due to

topographic shape. The frequency of amplification at M2 and M3 and valley station M4 appears to be the result of strong resonance that is consistent at each site, but which differs markedly between stations (~15 Hz at M2; ~10 Hz at M3; ~6 Hz at M4). More analyses are needed to better understand these particularly complex amplification patterns.

In summary, our initial analyses reveal significant complexity in ground motion amplification and polarization over small distances within our arrays for any given event. Our work supports the hypothesis that local topographic-related effects strongly influence ground motion in hillside areas of highly variable topography. Our preliminary analyses of the Kinsey Terrace data also suggests that the nature and structure of the slope forming materials can also influence the amplification and directivity of ground motions. This has implications for engineering applications, given that all stations under investigation are classed as rock according to the New Zealand design standards (NZS1170).

Ongoing work will include in-depth spectral analyses from all array datasets to isolate topographic site effects and understand how they may vary during different strengths of shaking or incoming wave direction. It is also worth mentioning our recent initiative in conjunction with GeoNet to install two permanent GeoNet strong motion boreholes sites (each equipped with a downhole and a surface sensor) located in the neighbourhoods of Richmond Hill and Redcliffs. These borehole sensors will allow greater insight into ground motion effects occurring in the shallow subsurface.

REFERENCES

Bell, D.H. & Trangmar, B.B. 1987. Regolith materials and erosion processes on the Port Hills. *Urban Slope Stability,* New Zealand Geomechanical Society: 93 – 105.

Bonamasa, O. and J.E Vidale (1991). Directional site resonances observed from aftershocks of the 18 October 1989 Loma Prieta earthquake. Bulletin of the Seismological Society of America 81(5): 1945-1957.

Buech, F., Davies, T.R., Pettinga, J.R. (2010). The Little Red Hill seismic experimental study: Topographic effects on ground motion at a bedrock-dominated mountain ediface. Bulletin of the Seismological Society of America 100(5A): 2219-2229.

Burjánek, J., G. Gassner-Stamm, V. Poggi, J.R. Moore (2010). Ambient vibration analysis of an unstable mountain slope. Geophysical Journal International 180: 820-828.

Del Gaudio, V. and J. Wasowski (2010). Advances and problems in understanding the seismic response of potentially unstable slopes. Engineering Geology, doi:10.1016/j.enggeo.2010.09.007.

Forsyth, P.J., D.J.A. Barrell, and R. Jongens (2008). Geology of the Christchurch area. Institute of Geological & Nuclear Sciences Limited, 1:250000 geological map 16: 1 sheet + 67 p.

Harp, E.L., and R.W. Jibson (2002). Anomalous concentrations of seismically triggered rock falls in Pacoima Canyon: Are they caused by highly susceptible slopes or local amplification of seismic shaking?. Bulletin of the Seismological Society of America 92(8): 3180-3189.

Hough, S.E.; J.R. Altidor, D. Anglade, D. Given, M.G. Janvier, J.Z. Maharrey, M. Meremonte, B.S. Mildor, C. Prepetit, and A. Yong (2010). Localized damage caused by topographic amplification during the 2010 M 7.0 Haiti earthquake. Nature Geoscience 3(11): 778-782.

Meunier, P., N. Hovius, and J.A. Haines (2008). Topographic site effects and the location of earthquake induced landslides. Earth and Planetary Science Letters 275: 221-232.

Sepúlveda, S.A.; W. Murphy, R.W. Jibson, D.N. Petley, (2005). Seismically induced rock slope failures resulting from topographic amplification of strong ground motions: The case of Pacoima Canyon, California. Engineering Geology 80: 336-348.

Standards New Zealand 2004. Structural Design Actions – Part 5 Earthquake Actions – New Zealand. New Zealand Standard NZS 1170.5:2004.

Acknowledgements

The authors would like to thank GeoNet technicians Lara Bland, Caroline Little, Charlie O'Reilly, Todd Chandler and John Young, as well as Tim O'Neil from Christchurch for their excellent and efficient help managing the arrays and installing the borehole stations. We also thank Stephen Bannister and Stuart Read for their constructive reviews of this manuscript. This work is supported by EQC through the grant 12/626.